THE JOURNAL OF PHYSICAL CHEMISTRY A

Article

Cite This: J. Phys. Chem. A 2019, 123, 4104−4118

pubs.acs.org/JPCA

Combined Experimental and Computational Study on the Reaction Dynamics of the 1-Propynyl (CH_3CC)−1,3-Butadiene ($CH_2CHCHCH_2$) System and the Formation of Toluene under Single Collision Conditions

Published as part of The Journal of Physical Chemistry virtual special issue "Hanna Reisler Festschrift".

Aaron M. Thomas,[†] Chao He,[†] Long Zhao,[†] Galiya R. Galimova,[‡,§] Alexander M. Mebel,*[,‡] and Ralf I. Kaiser*[,†]

[†]Department of Chemistry, University of Hawai'i at Manoa, Honolulu, Hawaii 96822, United States

[‡]Department of Chemistry and Biochemistry, Florida International University, Miami, Florida 33199, United States

[§]Samara National Research University, Samara 443086, Russia

Supporting Information

ABSTRACT: The crossed beams reactions of the 1-propynyl radical (CH_3CC; X^2A_1) with 1,3-butadiene ($CH_2CHCHCH_2$; X^1A_g), 1,3-butadiene-d_6 ($CD_2CDCDCD_2$; X^1A_g), 1,3-butadiene-d_4 ($CD_2CHCHCD_2$; X^1A_g), and 1,3-butadiene-d_2 ($CH_2CDCDCH_2$; X^1A_g) were performed under single collision conditions at collision energies of about 40 kJ mol^{-1}. The underlying reaction mechanisms were unraveled through the combination of the experimental data with electronic structure calculations at the CCSD(T)-F12/cc-pVTZ-f12//B3LYP/6-311G(d,p) + ZPE(B3LYP/6-311G(d,p) level of theory along with statistical Rice−Ramsperger−Kassel−Marcus (RRKM) calculations. Together, these data suggest the formation of the thermodynamically most stable C_7H_8 isomer—toluene ($C_6H_5CH_3$)—via the barrierless addition of 1-propynyl to the 1,3-butadiene terminal carbon atom, forming a low-lying C_7H_9 intermediate that undergoes multiple isomerization steps resulting in cyclization and ultimately aromatization following hydrogen atom elimination. RRKM calculations predict that the thermodynamically less stable isomers 1,3-heptadien-5-yne, 5-methylene-1,3-cyclohexadiene, and 3-methylene-1-hexen-4-yne are also synthesized. Since the 1-propynyl radical may be present in cold molecular clouds such as TMC-1, this pathway could potentially serve as a carrier of the methyl group incorporating itself into methyl-substituted (poly)acetylenes or aromatic systems such as toluene via overall exoergic reaction mechanisms that are uninhibited by an entrance barrier. Such pathways are a necessary alternative to existing high energy reactions leading to toluene that are formally closed in the cold regions of space and are an important step toward understanding the synthesis of polycyclic aromatic hydrocarbons (PAHs) in space's harsh extremes.

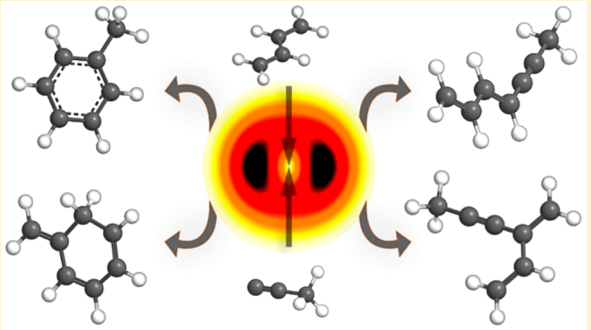

1. INTRODUCTION

Since its first isolation in 1837,[1] toluene ($C_6H_5CH_3$), **1** (Scheme 1), has been closely related to energetic materials where it was exploited in the synthesis of 2,4,6-trinitrotoluene (TNT)[2] and is added to gasoline to enhance fuel performance in combustion engines.[3] It is further recognized as a potential health and environmental hazard due to its role in the formation of polycyclic aromatic hydrocarbons (PAHs)[4] and is of considerable interest to the combustion and astrochemistry communities. Here, PAHs and their derivatives are important intermediates in the production of terrestrial soot and carbonaceous grains in circumstellar envelopes such as of the dying carbon star IRC+ 10216.[5,6]

In these environments, high temperatures cause toluene to form the benzyl ($C_6H_5CH_2$) moiety—an aromatic (AR) *and* resonantly stabilized free radical (RSFR)—by unimolecular decomposition or hydrogen abstraction reactions from the

Scheme 1. Reaction Path from Toluene (C_7H_8), 1, to Indene (C_9H_8), 4

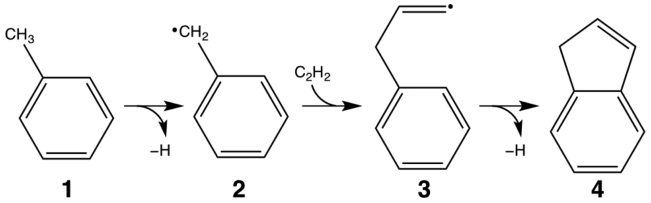

Received: January 4, 2019
Revised: April 13, 2019
Published: April 24, 2019

DOI: 10.1021/acs.jpca.9b00092
J. Phys. Chem. A 2019, 123, 4104−4118

methyl group.[7,8] While historical descriptions of PAH growth in combustion and astrophysical systems rely on the presence of a monocyclic aromatic hydrocarbon precursor such as benzene (C_6H_6) or phenyl (C_6H_5),[9−13] the chemistry of RSFRs and their role in mass growth processes have gained traction in both communities.[14] The benzyl radical, for example, has been proposed to form PAHs carrying fused benzene rings such as naphthalene ($C_{10}H_8$) via reactions with the propargyl (CH_2CCH) radical[15] and phenanthrene ($C_{14}H_{10}$) by self-reaction.[16,17] Indene (C_9H_8), the simplest PAH, comprising one six- and one five-membered ring, has been identified among the products of toluene pyrolysis.[4,18] The reaction mechanism likely begins with the formation of benzyl (**2**), followed by acetylene (C_2H_2) addition to form 3-phenylallyl, **3** ($C_6H_5C_3H_4$), which undergoes ring closure followed by hydrogen atom loss to yield indene (C_9H_8), **4** (Scheme 1).[19] Although the reaction is overall exoergic, the entrance barrier is rather large, depicting 51 kJ mol^{-1}, and it can therefore not be overcome at low temperatures such as in cold molecular clouds like the Taurus Molecular Cloud (TMC-1); however, this pathway may be relevant in high temperature settings like circumstellar envelopes of carbon stars.[20,21] Indene can be further processed into more complex PAHs, resulting in a strained carbon skeleton in acenaphthylene, **5** ($C_{12}H_8$), and curvature in corannulene, **6** ($C_{20}H_{10}$) (Figure 1).[22] These PAHs are considered

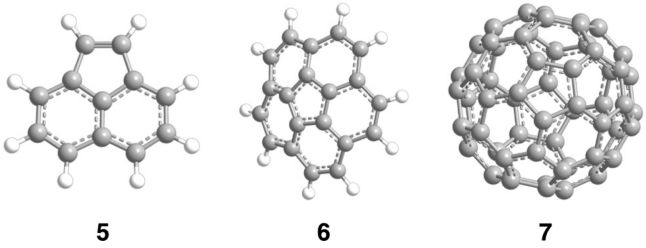

Figure 1. Acenaphthylene ($C_{12}H_8$), **5**, corannulene ($C_{20}H_{10}$), **6**, and buckminsterfullerene (C_{60}), **7**.

intermediates in the synthesis of fullerenes like buckminsterfullerene (C_{60}), **7**, under combustion conditions;[23] the large dipole moments of **5** and **6** of 0.30 and 2.19 D make them ideal candidates for detection in the interstellar medium (ISM).[24]

However, the information on the formation mechanisms for toluene is very limited. Toluene has been suggested to be synthesized via reactions of benzene (C_6H_6) plus methyl (CH_3) via a barrier of 54 kJ mol^{-1} or via hydrogen atom addition to the benzyl radical;[25,26] toluene was recently identified as a reaction product of the gas-phase reaction of ethynyl-*d* (C_2D) with isoprene (C_5H_8) under single-collision conditions.[27] In the present work, we access the C_7H_9 potential energy surface experimentally under single collision conditions and computationally, and we reveal a *barrierless* pathway to toluene via the reaction of the 1-propynyl (CH_3CC) radical with 1,3-butadiene ($CH_2CHCHCH_2$). Owing to its barrierless nature, this reaction can proceed in cold, dense regions of the ISM, such as found within TMC-1 with average molecular translational temperatures of 10 K, hence providing a nontraditional, hitherto neglected route to precursors such as toluene as molecular building block, leading eventually to PAHs carrying a five-membered ring like indene.

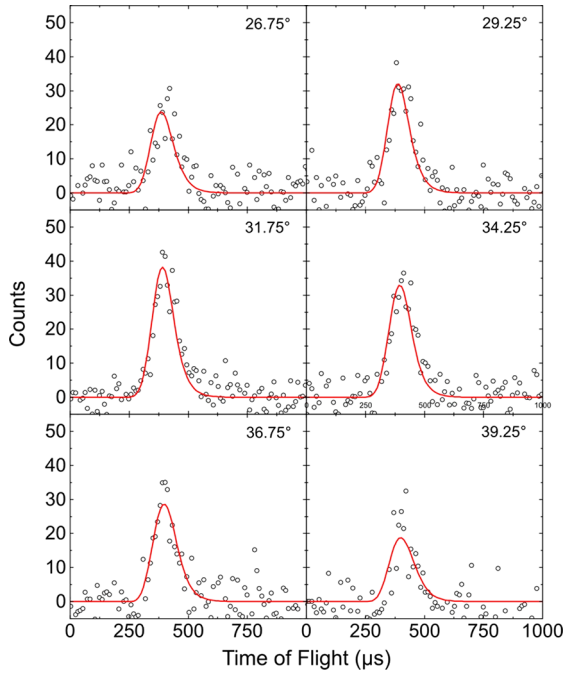

Figure 2. Time-of-flight data (TOF) recorded at m/z 91 ($C_7H_7^+$) for the reaction of the 1-propynyl (CH_3CC; X^2A_1) radical with 1,3-butadiene ($CH_2CHCHCH_2$; X^1A_g). The circles represent the experimental data and the red lines the fit.

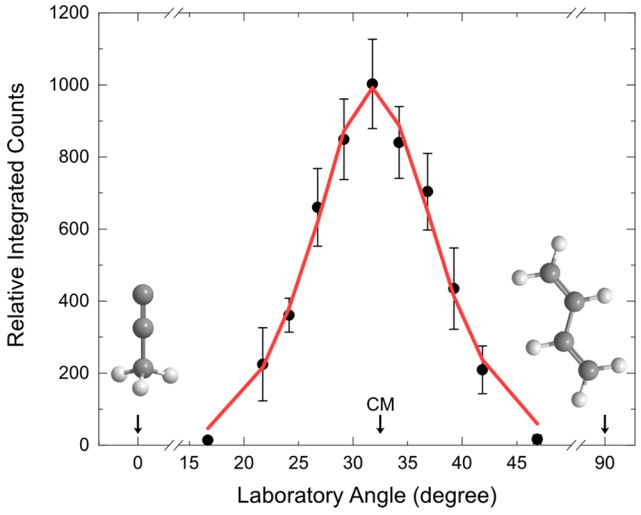

Figure 3. Laboratory angular distribution obtained at m/z 91 ($C_7H_7^+$) from the reaction of the 1-propynyl (CH_3CC; X^2A_1) radical with 1,3-butadiene ($CH_2CHCHCH_2$; X^1A_g).

2. EXPERIMENTAL AND COMPUTATIONAL METHODS

2.1. Experimental Methods. The 1-propynyl radical (CH_3CC; X^2A_1) reactions with 1,3-butadiene ($CH_2CHCHCH_2$; X^1A_g) and its isotopologues were conducted under single-collision conditions using a crossed molecular beams machine at the University of Hawaii.[28−33] A pulsed beam of 1-propynyl radicals was produced by photodissociation (193 nm; 20 mJ pulse^{-1}) of 1-iodopropyne (CH_3CCI; TCI, 98%) diluted at a level of 0.5% in helium (He, 99.9999%; Airgas),[34] then skimmed and velocity selected using a four-slot chopper wheel that resulted in a well-defined peak velocity v_p of 1713 ± 29 m s^{-1} and speed ratio S of 6.8 ± 0.6. These radicals intercepted a

DOI: 10.1021/acs.jpca.9b00092
J. Phys. Chem. A 2019, 123, 4104−4118

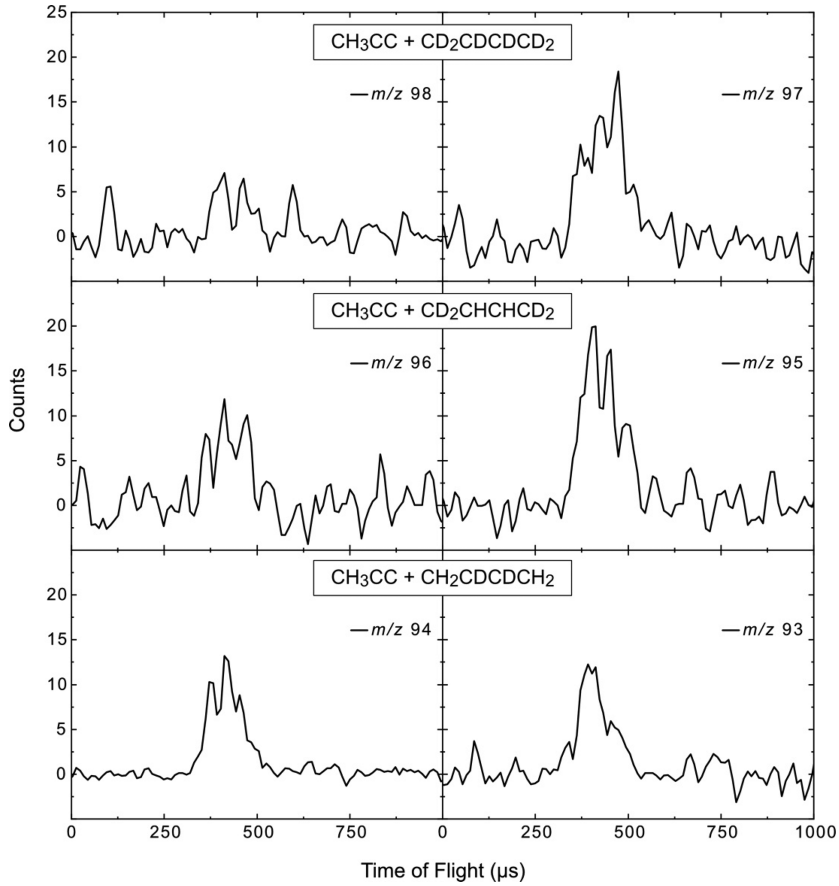

Figure 4. Time-of-flight data for the reaction of the 1-propynyl (CH_3CC) radical with (top) 1,3-butadiene-d_6 ($CD_2CDCDCD_2$), (middle) 1,3-butadiene-1,1,4,4-d_4 ($CD_2CHCHCD_2$), and (bottom) 1,3-butadiene-2,3-d_2 ($CH_2CDCDCH_2$).

neat 1,3-butadiene (Aldrich Chemistry, ≥99%) pulsed molecular beam (v_p = 777 ± 12 m s^{-1}, S = 9.5 ± 0.3), triggered 90 μs prior to the primary pulsed valve trigger, perpendicularly in the reaction chamber with a mean collision energy of 40 ± 1 kJ mol^{-1}. Experiments with (partially) deuterated reactants were performed using 1,3-butadiene-2,3-d_2 ($CH_2CDCDCH_2$; CDN Isotopes, 98.8% atom D), 1,3-butadiene-1,1,4,4-d_4 ($CD_2CHCHCD_2$; Cambridge Isotopes, 98% atom D), and 1,3-butadiene-d_6 ($CD_2CDCDCD_2$; Cambridge Isotopes, 98% atom D) to identify the position of the hydrogen and/or deuterium loss. The neutral products of the reactive scattering process were ionized at 80 eV, filtered according to mass-to-charge (m/z) ratio, and then detected using a Daly-type particle detector. Angularly resolved time-of-flight (TOF) spectra were recorded in the plane of the reactant beams at discrete laboratory angles, which were integrated to extract the laboratory angular distribution. The experimental data were fit using a forward-convolution routine[35] that is constrained by the reactant beam divergences, velocity spreads, and various machine parameters.[36,37] This represents an iterative method whereby user defined center-of-mass (CM) translational energy $P(E_T)$ and angular $T(\theta)$ flux distributions are varied until a suitable fit of the laboratory-frame TOF spectra and angular distributions are achieved. The CM functions comprise the reactive differential cross section $I(\theta, u)$, which is taken to be separable into its CM scattering angle θ and CM velocity u components, $I(u, \theta) \sim P(u) \times T(\theta)$.

2.2. Computational Methods. Geometries of the reactants, intermediates, transition states, and products of the

Scheme 2. Reactant and Product Mass Combinations in the Reactions of 1-Propynyl with (a) 1,3-Butadiene-d_6 ($CD_2CDCDCD_2$), (b) 1,3-Butadiene-1,1,4,4-d_4 ($CD_2CHCHCD_2$), and (c) 1,3-Butadiene-2,3-d_2 ($CH_2CDCDCH_2$)

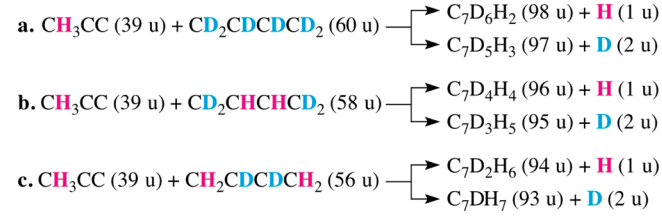

1-propynyl radical (CH_3CC; X^2A_1) reactions with 1,3-butadiene ($CH_2CHCHCH_2$; X^1A_g) were optimized at the density functional B3LYP/6-311G(d,p) level of theory.[38,39] Vibrational frequencies were computed at the same theoretical level and were used for the evaluation of zero-point vibrational energy corrections (ZPE) and in calculations of rate constants. Energies were refined by single-point calculations using the explicitly correlated coupled clusters CCSD(T)-F12 method[40,41] with Dunning's correlation-consistent cc-pVTZ-f12 basis set.[42,43] The expected accuracy of the CCSD(T)-F12/cc-pVTZ-f12// B3LYP/6-311G(d,p) + ZPE(B3LYP/6-311G-(d,p)) relative energies is within 4 kJ mol^{-1} or better.[44] The ab initio calculations were performed using the GAUSSIAN 09[45] and MOLPRO 2010[43] program packages. Rate constants of all pertinent unimolecular reaction steps on the C_7H_9 PES following initial association of the 1-propynyl radical with

DOI: 10.1021/acs.jpca.9b00092
J. Phys. Chem. A 2019, 123, 4104−4118

1,3-butadiene were computed using Rice−Ramsperger−Kassel−Marcus (RRKM) theory,[46−48] as functions of available internal energy of each intermediate or transition state, where numbers and densities of states were obtained within the harmonic approximation using B3LYP/6-311G(d,p) computed frequencies. RRKM rate constants were utilized to compute product branching ratios by solving first-order kinetic equations within steady-state approximation.[49]

3. RESULTS

3.1. Laboratory Frame. Reactive scattering signal from the reaction of the 1-propynyl (CH_3CC; X^2A_1) radical with 1,3-butadiene ($CH_2CHCHCH_2$; X^1A_g) was observed at mass-to-charge ratios (m/z) 93, 92, and 91 with the latter signal having a better signal-to-noise ratio. These TOF spectra were found to be superimposable after scaling and therefore originate from the atomic hydrogen (H) loss channel forming C_7H_8 product(s) that are singly or dissociatively ionized to populate m/z 92 ($C_7H_8^+$) and m/z 91 ($C_7H_7^+$), respectively, alongside $^{13}CC_6H_8$ giving a signal at m/z 93 at a level less than 7.7% due to the natural abundance of the ^{13}C isotope of carbon. The time-of-flight (TOF) spectra of $C_7H_7^+$ were recorded in discrete angular intervals of 2.5° and fit using a product mass combination of 92 amu (C_7H_8) plus 1 amu (H). Selected TOF spectra are shown in Figure 2, and the corresponding laboratory angular distribution of the C_7H_8 product(s) is depicted in Figure 3 with the fit overlaid on the experimental data. Notable features of the laboratory angular distribution include its breadth of about 30° and its symmetry about the center-of-mass (CM) angle (32.1 ± 0.6°), which together suggest that C_7H_8 is produced in an indirect reaction via a complex formation involving one or more C_7H_9 intermediates.

Combined, the 1-propynyl and 1,3-butadiene reactants possess three sets of chemically inequivalent hydrogen atoms that, by use of isotopic labeling, can be traced into the product channel(s) and therefore enhance the interpretation of the experimental data. Additional experiments were therefore conducted using isotopologues of 1,3-butadiene replacing the C1−C4 (1,3-butadiene-d_6; 60 u), C1/C4 (1,3-butadiene-1,1,4,4-d_4; 58 u), and C2/C3 (1,3-butadiene-2,3-d_2; 56 u) hydrogen atoms with deuterium (D) (Figure 4). With the CH_3CC plus C_4H_6 reactive scattering signal determined to arise solely from the atomic hydrogen loss channel, the isotopologues can be used to further assess from which reactant(s) and thus functional group(s) the loss originates since H-loss and D-loss products have distinct masses (Scheme 2). The CH_3CC plus 1,3-butadiene-d_6 reaction can therefore form $C_7D_6H_2$ (98 u) plus H (1 u) and/or $C_7D_5H_3$ (97 u) plus D (2 u). We monitored for singly ionized reaction products at m/z 98 ($C_7D_6H_2^+$) and m/z 97 ($C_7D_5H_3^+$) and detected reactive scattering signal at each mass-to-charge ratio. Accounting for fragmentation of $C_7D_6H_2$ to $C_7D_6H^+$ (m/z 97) by electron impact and the appearance of $^{13}CC_6D_5H_3^+/^{13}CC_6D_6H^+$ at m/z 98, we find that both $C_7D_6H_2$ and $C_7D_5H_3$ are formed at fractions of 24 ± 10% and 76 ± 10%, respectively. For the CH_3CC plus 1,3-butadiene-1,1,4,4-d_4 reaction, the potential products are $C_7D_4H_4$ (96 u) plus H (1 u) and $C_7D_3H_5$ (95 u) plus D (2 u). We therefore monitored for reaction products at m/z 96 and m/z 95 and observed reactive scattering signal at each mass-to-charge ratio. Accounting for the natural distribution of ^{13}C and the effects of dissociative ionization, the formation of both $C_7D_4H_4$ and $C_7D_3H_5$ was found to account for the observed signal with branching ratios of 45 ± 10% and 55 ± 10%, respectively. Lastly, in the CH_3CC plus 1,3-butadiene-2,3-d_2 reaction, the possible reaction products are $C_7D_2H_6$ (94 u) plus H (1 u) and C_7DH_7 (93 u) plus D (2 u); we therefore probed and observed reactive scattering signal at both m/z 94 and m/z 93 from which we determined 90 ± 10% is due to the formation of $C_7D_2H_6$ while 10 ± 10% is due to C_7DH_7. In summary, we find that in the CH_3CC plus $CD_2CDCDCD_2$, $CD_2CHCHCD_2$, and $CH_2CDCDCH_2$ reactions, the atomic hydrogen (H) loss accounts for 24 ± 10%, 45 ± 10%, and 90 ± 10% of the total product signal, with the remaining yield attributed to atomic deuterium (D) loss.

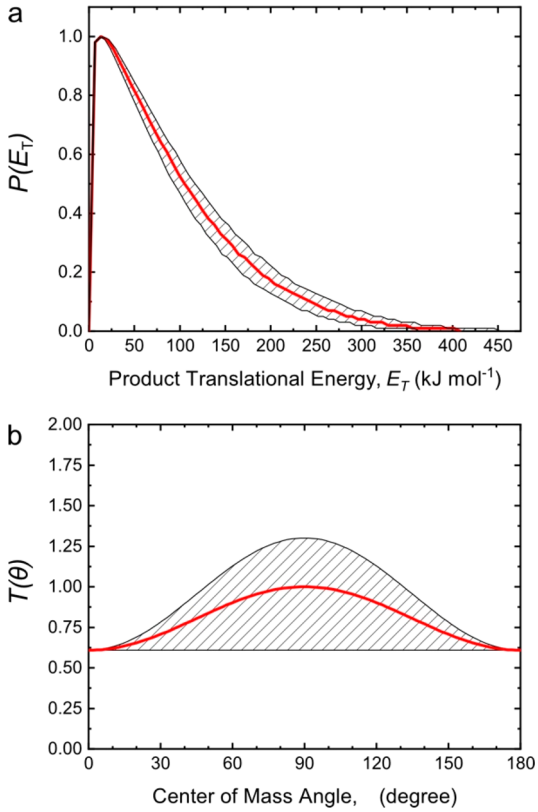

Figure 5. Center-of-mass translational energy (a) and angular (b) flux distributions for the formation of C_7H_8 plus atomic hydrogen via the reaction of the 1-propynyl (CH_3CC; X^2A_1) radical with 1,3-butadiene ($CH_2CHCHCH_2$; X^1A_g). (Hatched areas) Regions of acceptable fits.

How can these data be exploited to elucidate the position(s) of the hydrogen and/or deuterium loss(es)? First, the $CH_3CC/CD_2CDCDCD_2$ system (Scheme 2a) probed explicitly the hydrogen atom loss from the methyl group of the 1-propynyl radical via m/z = 94; this is the *only* source of hydrogen atoms in this reaction. The detection of the $C_7D_6H_2$ plus H channel therefore provides clear evidence that 24 ± 10% of the reaction products were formed by ejection of a hydrogen atom initially bound to the methyl group of the 1-proynyl reactant. Second, in the $CH_3CC/CD_2CHCHCD_2$ system (Scheme 2b), with the additional hydrogen atoms at the C2 and C3 carbon atoms, the yield of the H atom loss pathway increased slightly from 24 ± 10% (only from the CH_3 group) to 45 ± 10% (from the CH_3 and CH groups). This suggests that 21 ± 20% of the H atoms are lost from the CH moieties at the C2/C3 carbon atoms of the $CD_2CHCHCD_2$ reactant. Also, 55 ± 10% of products formed in the $CH_3CC/CD_2CHCHCD_2$ system were attributed to the formation of $C_7D_3H_5$ plus D, i.e., the D loss from the CD_2 moieties of the

DOI: 10.1021/acs.jpca.9b00092
J. Phys. Chem. A 2019, 123, 4104−4118

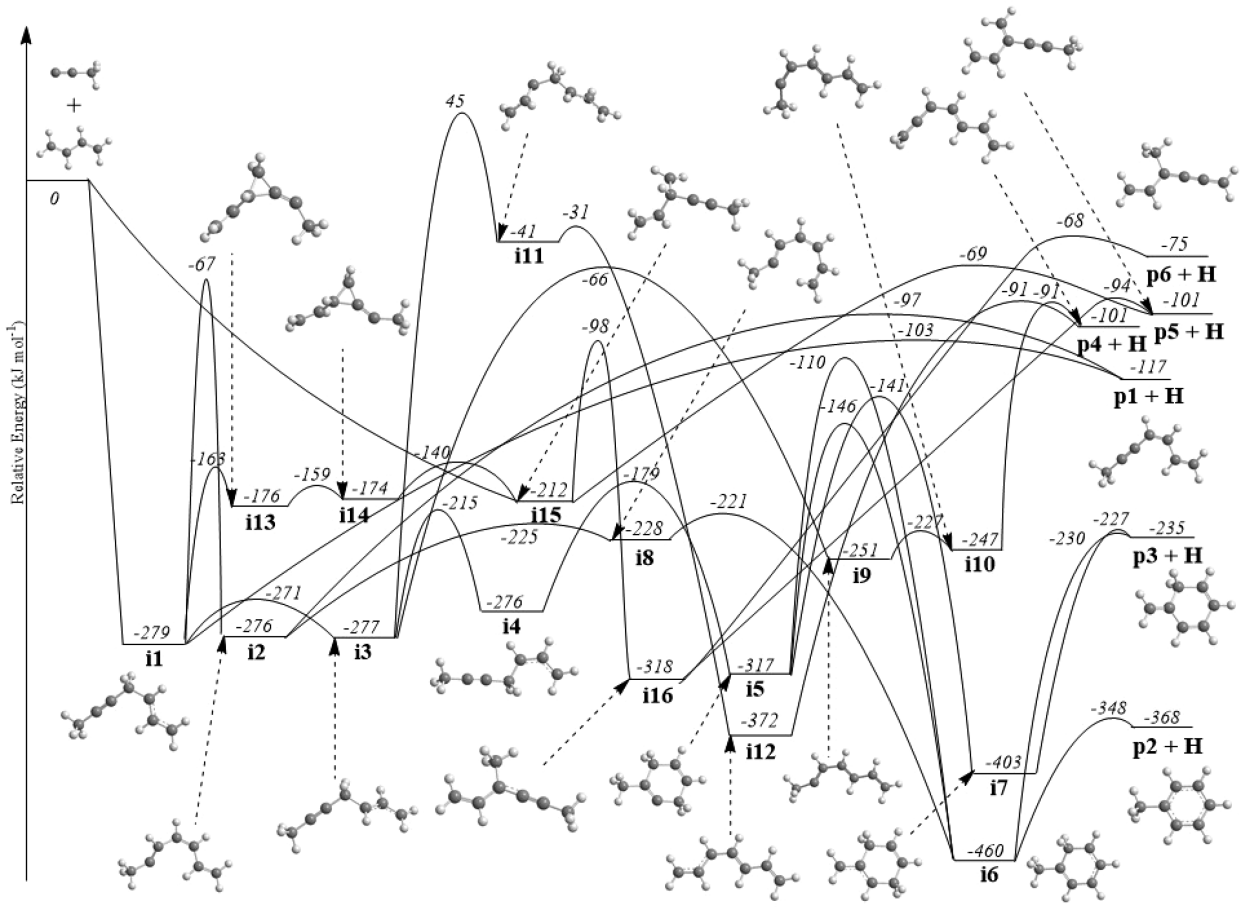

Figure 6. Potential energy surface for the bimolecular reaction of the 1-propynyl (CH_3CC; X^2A_1) radical with 1,3-butadiene ($CH_2CHCHCH_2$; X^1A_g) leading to C_7H_8 plus H products.

C1/C4 atoms. Finally, in the $CH_3CC/CH_2CDCDCH_2$ system, the combined H atom loss yield from the CH_3 group of the 1-propynyl radical and from CH_2 groups of the $CH_2CDCDCH_2$ reactant (Scheme 2c) accumulated to 90 ± 10%; considering that 24 ± 10% of the H atoms arise from the CH_3 group of the 1-propynyl radical (Scheme 2a), 66 ± 20% of the H atoms are released from the CH_2 groups of the $CH_2CDCDCH_2$ reactant (Scheme 2c). This number is consistent within the error limits with the D loss yield derived in the $CH_3CC/CD_2CHCHCD_2$ system (Scheme 2b) of 55 ± 10%. Overall, accounting for the aforementioned yields, we determine that, for the 1-propynyl−1,3-butadiene reaction, 24 ± 10% of the H atoms are released from the CH_3 group of the radical reactant with 61 ± 11% of the H atoms originating from the CH_2 group at the C1/C4 of the $CH_2CDCDCH_2$ reactant; the remaining balance of 15 ± 15% of the H loss can be attributed to the H emission from the CH groups at the C2/C3 of the 1,3-butadiene. Therefore, the laboratory data alone show that the 1-propynyl (CH_3CC) radical reacts with 1,3-butadiene (C_4H_6) to form at least two C_7H_8 isomers by emission of atomic hydrogen via indirect and overall exoergic reaction mechanisms. With the aid of isotopic labeling, atomic hydrogen emission was found to originate predominantly from 1,3-butadiene's methylene (CH_2) groups and from the 1-propynyl radical methyl group (CH_3) with possibly minor contributions from the methylidyne (CH) groups.

3.2. Center-of-Mass Frame. Having identified that the reaction product(s) carry the empirical formula C_7H_8 and that the hydrogen atoms are predominantly lost from the 1-propynyl methyl group and from the C1/C4 CH_2 moiety of 1,3-butadiene, we now extract information on the reaction mechanism with the goal of identifying which C_7H_8 isomer or isomers are formed in the reactive scattering experiment. The results of this analysis are the center-of-mass (CM) translational energy $P(E_T)$ and angular $T(\theta)$ flux distributions, shown in Figure 5. The $P(E_T)$ has a maximum energy cutoff of 408 ± 45 kJ mol^{-1}, which, considering the experimental collision energy of 40 ± 1 kJ mol^{-1}, suggests that products are formed in overall exoergic reactions of about 368 ± 46 kJ mol^{-1}. Note that the large error reflects the lack of sensitivity to the total available energy or the maximum translational energy for C_7H_8, due to the signal-to-noise ratio and the light hydrogen atom leaving the collision complex. The distribution holds a maximum near 20 ± 2 kJ mol^{-1} and corresponds to about 23 ± 3% of the total available energy being deposited into translational degrees of freedom. The relatively low fraction of energy used for translation of nascent C_7H_8 along with the away-from-zero translational energy peaking of the $P(E_T)$ suggests that the reaction proceeds to products indirectly via activated C_7H_9 intermediates that decompose via tight exit transition states. The indirect aspect of the reaction mechanism is corroborated by the derived $T(\theta)$ that is forward−backward symmetric and portrays nonzero intensity at all angles. The reaction products are likely sideways-scattered as indicated by the $T(\theta)$ distribution maximum occurring at 90°, which suggests geometrical constraints on the exit transition state where

DOI: 10.1021/acs.jpca.9b00092
J. Phys. Chem. A 2019, 123, 4104−4118

the hydrogen atom is emitted perpendicular to the rotational plane of the decomposing intermediate and parallel to the total angular momentum vector.[50,51]

4. DISCUSSION

4.1. Energetics. In the case of polyatomic systems, it is beneficial to merge the experimental data with electronic structure calculations to elucidate the reaction dynamics leading to C_7H_8 formation. The full potential energy surface (PES) along with 6 product isomers (**p1**−**p6**) and 16 intermediates (**i1**−**i16**) joined by 27 transition states is compiled in Figure 6, whereas computed geometries of the exit transition states leading to the formation of various C_7H_8 isomers are illustrated in Figure 7. Overall, the CH_3CC radical can add barrierlessly

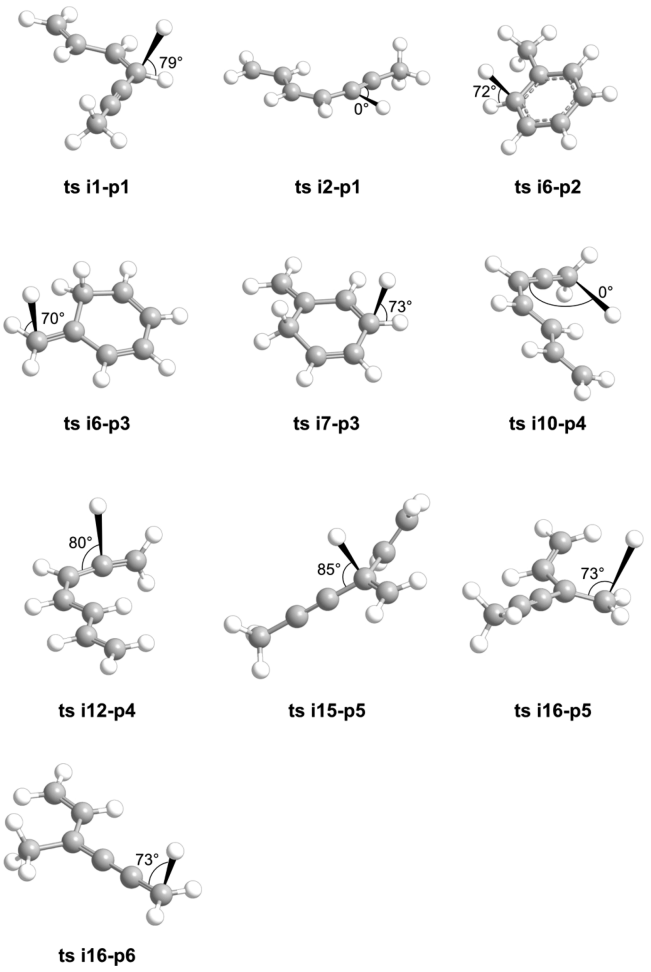

Figure 7. Computed geometries of the exit transition states leading to the formation of C_7H_8 isomers **p1**−**p6**. The angle for each departing hydrogen atom is given with respect to the rotation plane of the decomposing complex.

with its radical center at the carbon atom to the π system of 1,3-butadiene ($CH_2CHCHCH_2$) forming a covalent carbon−carbon single bond either to its C1/C4 (**i1**) or C2/C3 (**i15**) carbon atom. These intermediates are connected by a facile two-step isomerization via **i13** and **i14** involving ring closure and a 1,2-shift of the 1-propynyl group ultimately providing access—via varying steps of isomerization and/or hydrogen atom emission as discussed below—to at least six low-lying C_7H_8 isomers: 1,3-heptadien-5-yne (**p1** + H; −117 ± 4 kJ mol^{-1}), toluene (**p2** + H; −368 ± 4 kJ mol^{-1}), 5-methylene-1,3-cyclohexadiene (**p3** + H; −235 ± 4 kJ mol^{-1}), 1,2,4,6-hepatetraene (**p4** + H; −101 ± 4 kJ mol^{-1}), 3-methylene-1-hexen-4-yne (**p5** + H; −101 ± 4 kJ mol^{-1}), and 4-methyl-1,2,3,5-hexatetraene (**p6** + H; −75 ± 4 kJ mol^{-1}). Note that the experimental reaction energy to form the most thermodynamically favorable product toluene is −364 kJ mol^{-1} according to the standard enthalpies of formation at 0 K from *Active Thermochemical Tables*.[52] Which of these isomer(s) is actually formed under single collision conditions? To answer this question, we are now merging the experimental and theoretical data to gain ultimate insight into the underlying reaction dynamics of the 1-propynyl plus 1,3-butadiene reaction. The experimental data can be fit using a translational energy distribution that gives a reaction energy of −368 ± 46 kJ mol^{-1} and can therefore be rationalized by the formation of the aromatic C_7H_8 isomer toluene **p2**. However, the atomic hydrogen loss was found to originate predominantly from the methylene (CH_2) groups of 1,3-butadiene and from the methyl (CH_3) group of the 1-propynl radical; only minor contributions—if any—originate from the CH moiety of 1,3-butadiene as extracted through a series of experiments using isotopologues of 1,3-butadiene (Figure 4; Scheme 2). The laboratory data therefore highlight the presence multiple product channels that are not readily deconvoluted under our experimental conditions. By cross-referencing these results with the PES, we may further inform the extent to which products **p1**, **p3**, **p4**, **p5**, and/or **p6** are formed in our crossed molecular beams experiment.

4.2. Strongly Exoergic Channels. First, the formation of toluene **p2** is in agreement with the derived CM translational energy flux distribution resulting in a reaction energy (−368 ± 46 kJ mol^{-1}) that correlates nicely with the computed product channel (**p2** + H; −368 ± 4 kJ mol^{-1}). Toluene could be formed following the barrierless addition of CH_3CC to 1,3-butadiene resulting in **i1** (Figure 6). Intermediate **i1** can undergo rotation around a central C−C single bond (**i3**) then *cis*−*trans* (**i4**) isomerization followed by ring closure via formation of a 2,5-dihydro-*o*-tolyl radical (**i5**) lying 317 kJ mol^{-1} below the separated reactants. Intermediate **i5** is connected to **i6**—the global minimum on the C_7H_9 PES stabilized by 460 kJ mol^{-1} with respect to the separated reactants—which represents the precursor to toluene (**p2**) formation. Intermediate **i5** and **i6** are unusually linked by two different 1,2-H shift transition states resulting in barriers of 171 and 207 kJ mol^{-1} whose structures and energetics depend on ring puckering and the angle of the methyl group with respect to the six-carbon ring. Intermediate **i1** can alternatively undergo hydrogen migration from its central CH_2 group to form **i2** via a high energy barrier of 212 kJ mol^{-1}. *Cis*−*trans* isomerization carries **i2** into **i8** via a relatively low-lying transition state and then ultimately to intermediate **i6** that can decompose by loss of a hydrogen atom of the ring CH_2 group, resulting in aromatization and the formation of toluene (**p2**) via a tight exit transition state located 20 kJ mol^{-1} above the products. In summary, the toluene product can be formed via the following sequences: $CH_3CC + C_4H_6 \rightarrow$ **i1** $\rightarrow$ [**i2** $\rightarrow$ **i8**]/[**i3** $\rightarrow$ **i4** $\rightarrow$ **i5**] $\rightarrow$ **i6** $\rightarrow$ **p2** + H (Figure 6).

It is important to highlight that the experimental findings fully agree with this reaction mechanism. The computed exit geometry for the departing hydrogen atom in the **i6** $\rightarrow$ **p2** + H transition state is 72° with respect to the rotating plane of the decomposing complex (Figure 7) and is consistent with the

DOI: 10.1021/acs.jpca.9b00092
J. Phys. Chem. A 2019, 123, 4104−4118

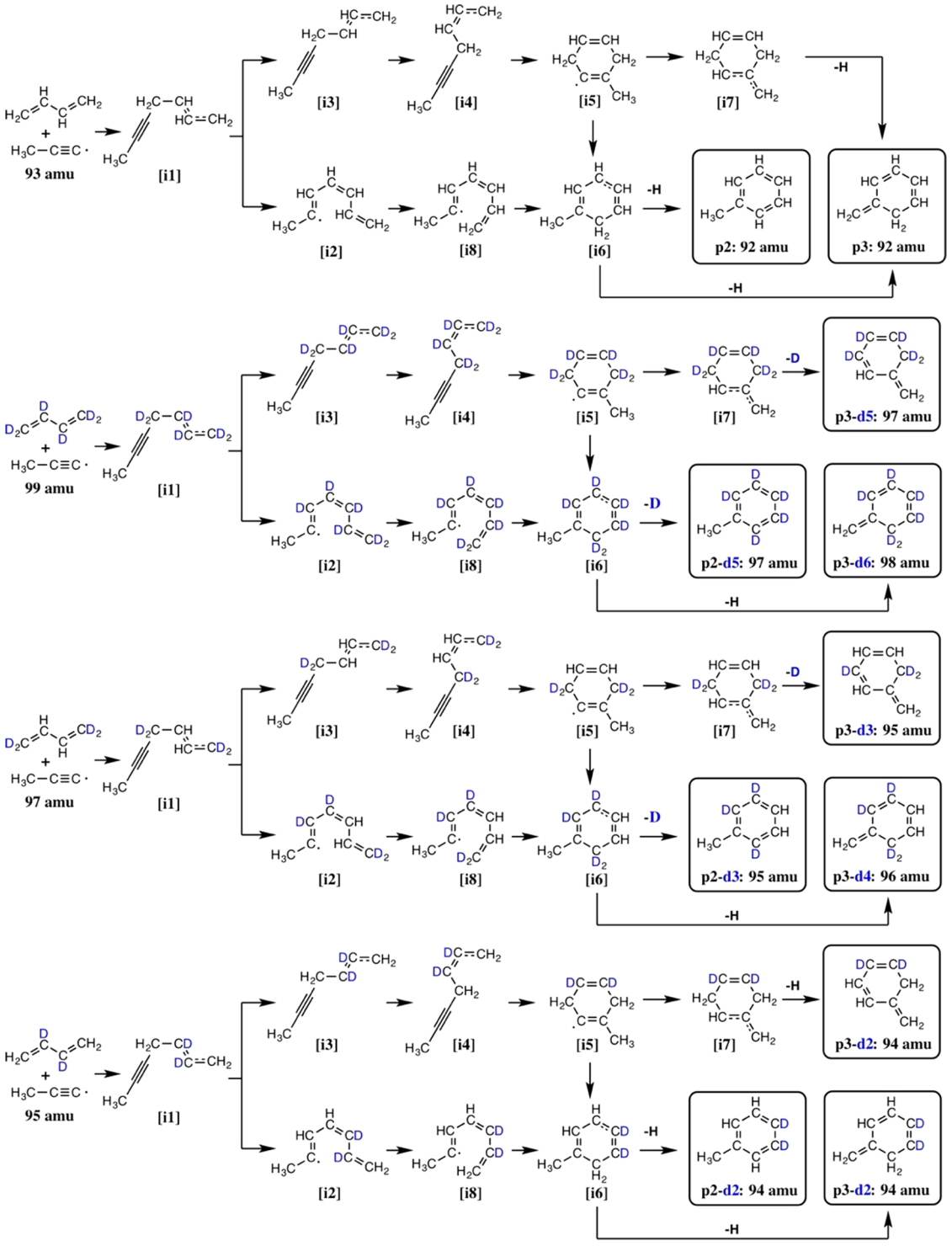

Figure 8. Reaction schematic for the bimolecular reaction of the 1-propynyl radical (CH_3CC; X^2A_1) radical with 1,3-butadiene-d_6 ($CD_2CDCDCD_2$), 1,3-butadiene-1,1,4,4-d_4 ($CD_2CHCHCD_2$), and 1,3-butadiene-2,3-d_2 ($CH_2CDCDCH_2$) leading to isotopologues of toluene (**p2**) and 5-methylene-1,3-cyclohexadiene (**p3**).

sideways scattering depicted in the $T(\theta)$ distribution. The computed exit barrier of 20 kJ mol^{-1} further agrees with the $P(E_T)$ whose maximum occurs near 20 kJ mol^{-1}. Further, the **i6** → **p2** + H pathway involves the emission of a hydrogen atom from the 1,3-butadiene's terminal methylene group; therefore, isotopologues of toluene should form by deuterium atom loss in the CH_3CC/C_4D_6 and $CH_3CC/C_4D_4H_2$ systems yielding **p2**-d_5 (97 amu; Scheme 2) and **p2**-d_3 (95 amu; Scheme 2), whereas the $CH_3CC/C_4D_2H_4$ system should give **p2**-d_2 (94 amu) by emission of a hydrogen atom (Figure 8). Indeed, we observed reactive scattering signals consistent with the formation of toluene and its d_5, d_3, and d_2 isotopologues and further determined that hydrogen-atom loss from 1,3-butadiene's methylene group(s) accounts for 61 ± 11% of the total product yield.

While the formation of 5-methylene-1,3-cyclohexadiene (**p3**) is less exoergic (−235 ± 4 kJ mol^{-1}) than the experimental

DOI: 10.1021/acs.jpca.9b00092
J. Phys. Chem. A 2019, 123, 4104−4118

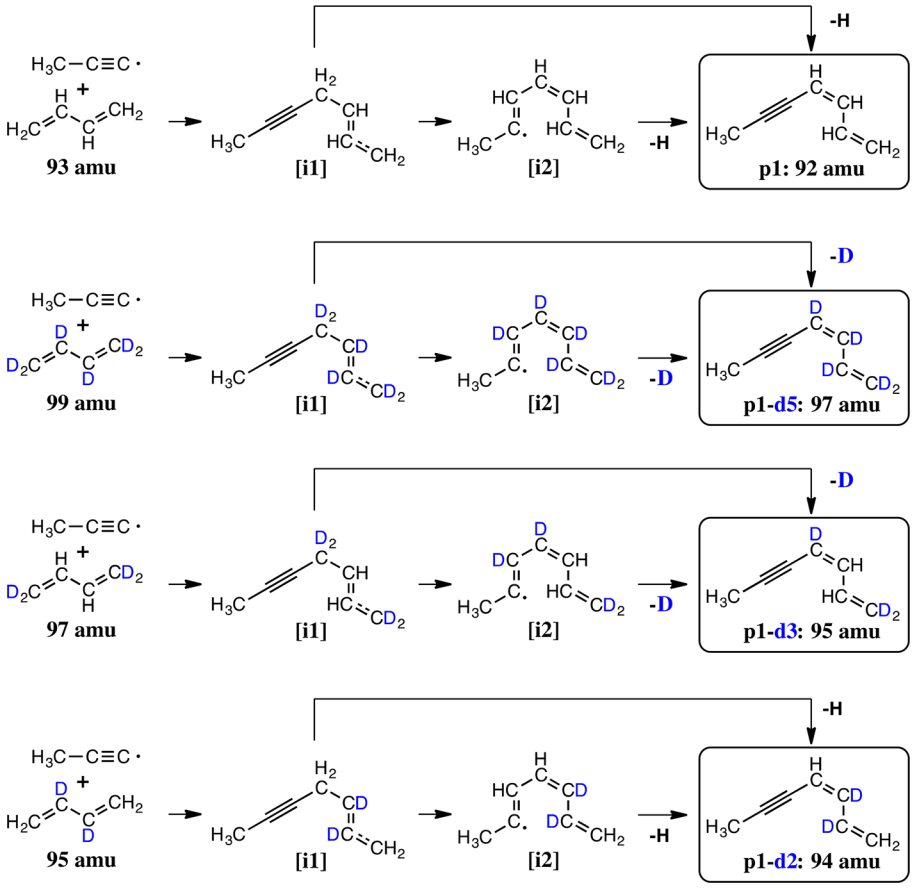

Figure 9. Reaction schematic for the bimolecular reaction of the 1-propynyl radical (CH_3CC; X^2A_1) radical with 1,3-butadiene-d_6 ($CD_2CDCDCD_2$), 1,3-butadiene-1,1,4,4-d_4 ($CD_2CHCHCD_2$), and 1,3-butadiene-2,3-d_2 ($CH_2CDCDCH_2$), leading to isotopologues of 1,3-heptadien-5-yne (**p1**).

high-energy product channel (-368 ± 46 kJ mol^{-1}), its presence among C_7H_8 products cannot be strictly excluded on the basis of reaction energetics alone where its identifying features could be masked in the low energy portion of the $P(E_T)$. The reaction pathways leading to **p3** are similar to those taken in the formation of toluene (**p2**). The cyclic intermediate **i5** can undergo hydrogen migration from the methyl substituent to the ring forming **i7**, which decomposes via emission of a ring hydrogen atom. Alternatively, **i5** can isomerize to **i6**, which then eliminates a methyl hydrogen atom to yield **p3** via a loose transition state located 5 kJ mol^{-1} above the product channel. The summary pathways to **p3** are thus $CH_3CC + C_4H_6$ → **i1** → [**i2** → **i8** → **i6**]/[**i3** → **i4** → **i5** → **i6**]/[**i3** → **i4** → **i5** → **i7**] → **p3** + H (Figure 6). The reaction exoergicity and exit-barrier height are not readily apparent in the high-energy $P(E_T)$. However, the computed exit geometries for **i6** → **p3** + H and **i7** → **p3** + H suggest the product would be also sideways scattered (Figure 7), where atomic hydrogen is emitted at angles of 70° and 73°, respectively, with respect to the rotational plane of the decomposing complex. If the **p3** + H channel is also accessed under our experimental conditions, it is not easily teased out of the isotopic data because it can be formed via **i6** by emission of a methyl hydrogen atom and by **i7** via emission of a ring hydrogen atom, where the emitted hydrogen atoms originate from 1-propynyl's methyl group and 1,3-butadiene's methylene group, respectively (Figure 8). Therefore, the CH_3CC plus C_4D_6 and CH_3CC plus $C_4D_4H_2$ reactions could form **p3** isotopologues via emission of atomic hydrogen (**p3**-d_6, **p3**-d_4) *and* atomic deuterium (**p3**-d_5, **p3**-d_3). In the CH_3CC-$C_4D_2H_4$ system, only **p3**-d_2 (94 amu) should form via hydrogen atom loss.

4.3. Weakly Exoergic Channels. On the C_7H_9 PES, **p1** can be formed from intermediate **i1** either by elimination of atomic hydrogen through an exit barrier 14 kJ mol^{-1} above the **p1** + H product channel, or following isomerization of **i1** to **i2**, which decomposes to **p1** + H via a relatively tight transition state 20 kJ mol^{-1} above the separated products. Isomer **p1** is thus formed via $CH_3CC + C_4H_6$ → **i1**/[**i1** → **i2**] → **p1** + H. The computed exit geometries for the departing hydrogen atom in **i1** → **p1** + H and **i2** → **p1** + H are 69° and 0° (Figure 7); i.e., elimination from **i1** is expected to occur almost perpendicularly to the plane of rotation, whereas elimination from **i2** occurs within the plane. The exit barriers to decomposition of **i1** and **i2** to form **p1** + H are 14 and 20 kJ mol^{-1}, respectively. Considering that intermediates **i1** and **i2** decompose by emitting a hydrogen atom from 1,3-butadiene's terminal methylene group, isotopologues of **p1** should form by deuterium atom loss in the $CH_3CC-C_4D_6$ and $CH_3CC-C_4D_4H_2$ systems, yielding **p1**-d_5 (97 amu) and **p1**-d_3 (95 amu) products, respectively, whereas the $CH_3CC-C_4D_2H_4$ system should form **p1**-d_2 by emission of a hydrogen atom (Figure 9). Reactive scattering signals were indeed observed in each reaction system, corresponding to light atom emission from the methylene groups of 1,3-butadiene.

Isomer **p4** can be formed via intermediate **i1** following isomerization to **i3**, from which there are two possible routes to **p4**. First is a low energy pathway proceeding from **i3** by a

DOI: 10.1021/acs.jpca.9b00092
J. Phys. Chem. A 2019, 123, 4104−4118

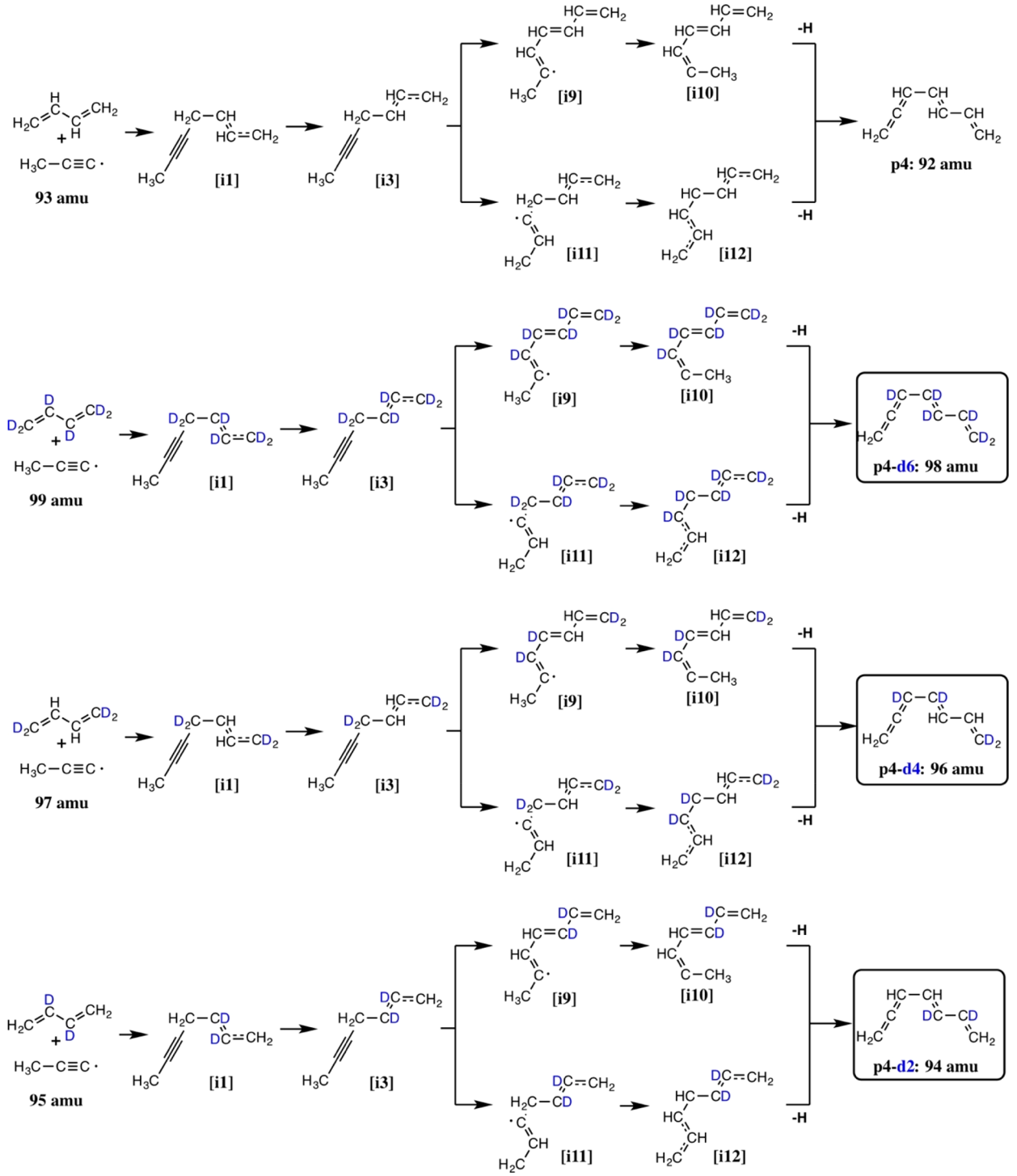

Figure 10. Reaction schematic for the bimolecular reaction of the 1-propynyl radical (CH_3CC; X^2A_1) radical with 1,3-butadiene-d_6 ($CD_2CDCDCD_2$), 1,3-butadiene-1,1,4,4-d_4 ($CD_2CHCHCD_2$), and 1,3-butadiene-2,3-d_2 ($CH_2CDCDCH_2$) leading to isotopologues of 1,2,4,6-hepatetraene (**p4**).

1,2-hydrogen migration from the methylene group toward the 1-propynyl moiety to form **i9**, followed by a repositioning of the methyl-group in a *trans*−*cis* isomerization over a 24 kJ mol^{-1} barrier to yield **i10**. The latter dissociates via hydrogen loss from the methyl group to form the cumulenic substituent in **p4** via a relatively loose exit transition state located 10 kJ mol^{-1} above the products. The second route involves hydrogen migration *from* the 1-propynl methyl group toward the 1,3-butadiene moiety to form **i11** over a high energy barrier located 45 kJ mol^{-1} above the separated reactants. The system undergoes then hydrogen migration from the methylene group to form a vinyl-substituted 1,3-butadiene (**i12**) that can ultimately eliminate its vinylic hydrogen atom to form **p4** via a loose exit transition state. In summary, the formation of isomer **p4** follows $CH_3CC + C_4H_6$ → **i1** → **i3** → [**i9** → **i10**]/[**i11** → **i12**] → **p4** + H. In the transition states connected to the **i10** → **p4** + H and **i12** → **p4** + H sequences, the departing hydrogen results at an angle of 0° and 80° (Figure 7), respectively. Regardless of the path taken

DOI: 10.1021/acs.jpca.9b00092
J. Phys. Chem. A 2019, 123, 4104−4118

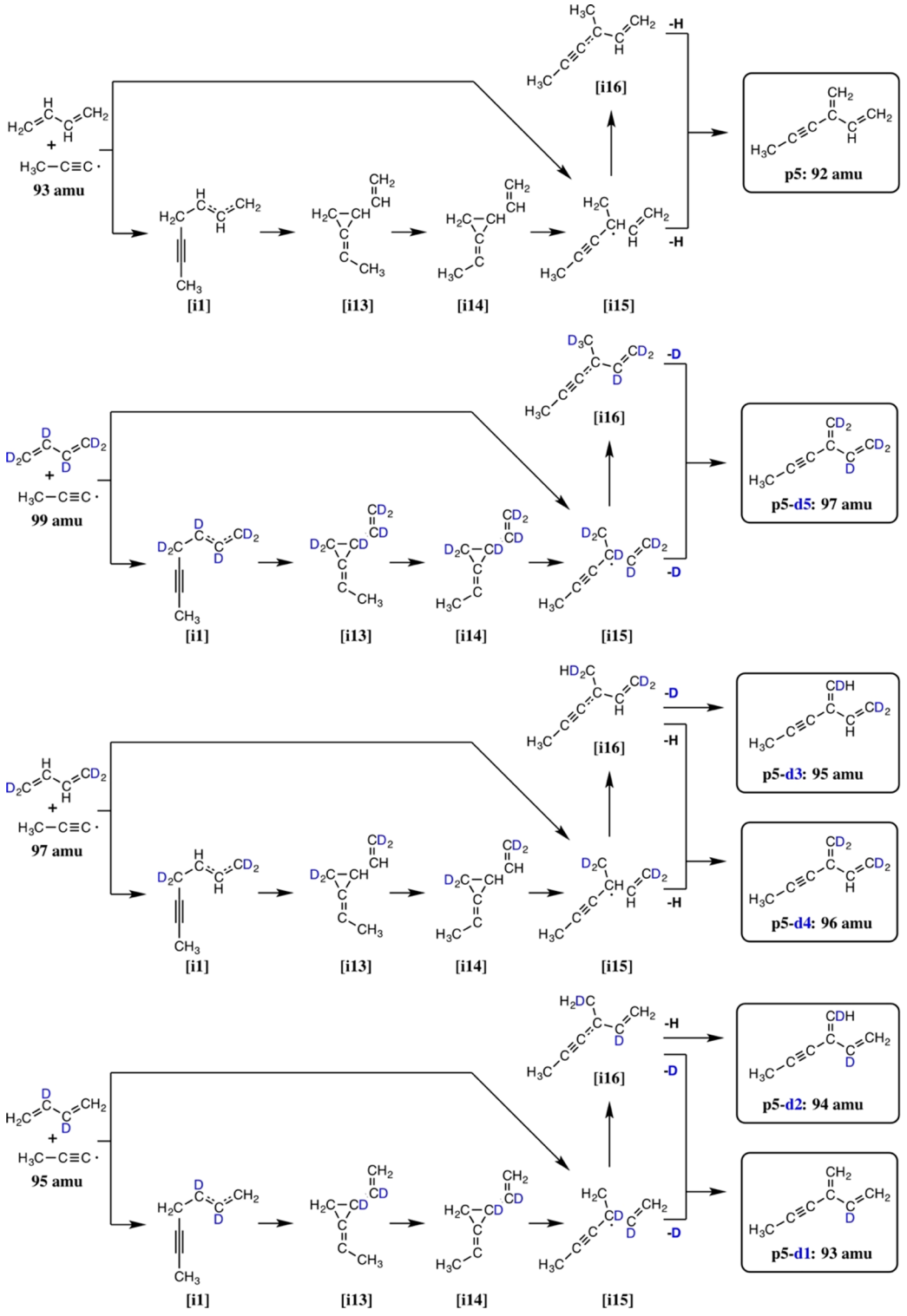

Figure 11. Reaction schematic for the bimolecular reaction of the 1-propynyl radical (CH_3CC; X^2A_1) radical with 1,3-butadiene-d_6 ($CD_2CDCDCD_2$), 1,3-butadiene-1,1,4,4-d_4 ($CD_2CHCHCD_2$), and 1,3-butadiene-2,3-d_2 ($CH_2CDCDCH_2$) leading to isotopologues of 3-methylene-1-hexen-4-yne (**p5**).

by the reactants, isomer **p4** is formed by emission of a hydrogen atom from 1-propynyl's methyl group, and thus isotopologues of **p4** formed in the $CH_3CC-C_4D_6$, $CH_3CC-C_4D_4H_2$, and $CH_3CC-C_4D_2H_4$ reaction systems are **p4**-d_6 (98 amu), **p4**-d_4 (96 amu), and **p4**-d_2 (94 amu), respectively, as shown in Figure 10. A reactive scattering signal was observed in each reaction system, corresponding to hydrogen atom emission from the methyl group of 1-propynyl at a level of 24 ± 10%.

Isomer **p5** can be formed via the entrance channel involving **i15**, resulting from the addition of 1-propynyl with its radical end to an interior carbon atom of 1,3-butadiene (C2/C3). Recall that the two entrance channels **i1** and **i15** are connected by intermediates **i13** and **i14**, which facilitate a 1,2-shift of the

DOI: 10.1021/acs.jpca.9b00092
J. Phys. Chem. A 2019, 123, 4104−4118

1-propynyl group through a ring closing/ring opening mechanism. Intermediate **i15** can eliminate atomic hydrogen to form **p5** via a tight exit transition state or isomerize to **i16** by surmounting a 114 kJ mol^{-1} barrier resulting in the formation of a new methyl group that emits a hydrogen atom to form **p5** via a relatively loose exit transition state of 7 kJ mol^{-1}. In summary, isomer **p5** can be formed via the following pathways: $CH_3CC + C_4H_6 \rightarrow$ [**i1** → **i13** → **i14** → **i15**]/[**i1** → **i13** → **i14** → **i15** → **i16**] → **p5** + H, or by $CH_3CC + C_4H_6 \rightarrow$ **i15**/[**i15** → **i16**] → **p5** + H. The calculated exit geometries for **i15** → **p5** + H and **i16** → **p5** + H indicate that atomic hydrogen is emitted at angles of 85° and 73° (Figure 7). Considering the isotopic experiments, the emitted hydrogen atoms can be clearly traced from 1,3-butadiene's methylidyne (CH/CD) groups in the case of the **i15** → **p5** pathway (Figure 11). However, recall that product formation via light atom emission from the methylidyne group(s) of 1,3-butadiene is minor. Alternatively, if **p5** forms from **i16**, the leaving H/D atom can originate both from the methylidyne or methylene groups in 1,3-butadiene with a statistical ratio of 1/2.

Lastly, the formation of isomer **p6** occurs on the PES similarly to that of **p5** with a departure occurring at **i16** via the emission of a hydrogen atom from the 1-propynyl group, resulting in the formation of a cumulenic substituent following rearrangement of the π electrons. The exit barrier is 250 kJ mol^{-1} and lies only 7 kJ mol^{-1} above the product channel. In summary, isomer **p6** can be formed via the following pathways: $CH_3CC + C_4H_6 \rightarrow$ [**i1** → **i13** → **i14** → **i15** → **i16**] → **p6** + H, or by $CH_3CC + C_4H_6 \rightarrow$ **i15** → **i16**] → **p6** + H. The calculated exit geometry for **i16** → **p6** + H indicates that atomic hydrogen is emitted at an angle of 73° (Figure 7). The formation of **p6** can only give a signal corresponding to hydrogen atom emission since isotopic labeling occurs only at the 1,3-butadiene reactant and **p6** is formed by loss of a hydrogen atom from the 1-propynyl group. In the absence of a ring closing step such as those occurring in the paths to **p2** and **p3**, isotopic scrambling with the 1-propynyl group is unlikely due to the absence of neighboring H/D atoms, and therefore, isotopologues of **p6** formed in the $CH_3CC-C_4D_6$, $CH_3CC-C_4D_4H_2$, and $CH_3CC-C_4D_2H_4$ reaction systems are **p6**-d_6 (98 amu), **p6**-d_4 (96 amu), and **p6**-d_2 (94 amu), respectively, as can be readily seen in Figure 11. A reactive scattering signal was observed in each reaction system, corresponding to hydrogen atom emission from the methyl group of 1-propynyl at a level of 24 ± 10%.

4.4. RRKM Calculations. Finally, we calculated the yield of the individual C_7H_8 product isomers using statistical RRKM theory (Table 1). In the zero-pressure limit and at a collision energy of 41 kJ mol^{-1}, isomers **p4** and **p6** are predicted to contribute less than 1% to the total C_7H_8 product yield, regardless of which entrance channel (**i1**/**i15**) is taken by the reactants. If the reaction begins with the formation of **i1**, isomer **p1** is the majority product with 57.9% of the C_7H_8 yield. The cyclic isomers **p2** and **p3**, along with **p5**, are formed preferentially when starting exclusively from **i1** with calculated yields of 15.5%, 11.4%, and 14.7%. At the other extreme beginning with **i15**, the yield of **p1** increases to 70.2% with all other abundances decreasing accordingly. The presence of **p5** among reaction products can be confirmed in the $CH_3CC/C_4D_2H_4$ system, where it was the only possible source of atomic deuterium loss products detected at a level of 10 ± 10%. If the reaction system behaves statistically, then the signature for **p3** can be found in the CH_3CC/C_4D_6 system,

Table 1. Statistical Branching Ratios (%) for the Reaction of the 1-Propynyl (CH_3CC) Radical with 1,3-Butadiene ($CH_2CHCHCH_2$) over a Range of Collision Energies E_C (kJ mol^{-1}) Following the Absolute Formation of C_7H_9 Intermediate i1 or i15[a]

	100% i1		0% i15			
E_C	p1	p2	p3	p4	p5	p6
0.00	36.0	32.2	23.2	0.1	8.4	0.1
10.46	43.1	26.9	19.5	0.1	10.3	0.1
20.92	49.1	22.3	16.2	0.2	12.1	0.1
31.38	54.1	18.4	13.5	0.2	13.5	0.2
41.10	57.9	15.5	11.4	0.3	14.7	0.3
41.84	58.2	15.3	11.2	0.3	14.8	0.3
52.30	61.4	12.8	9.4	0.4	15.8	0.3
	0% i1		100% i15			
E_C	p1	p2	p3	p4	p5	p6
0.00	52.2	23.3	16.8	0.1	7.5	0.1
10.46	59.0	18.4	13.3	0.1	9.0	0.1
20.92	64.1	14.5	10.6	0.1	10.5	0.1
31.38	67.8	11.5	8.4	0.1	11.9	0.2
41.10	70.2	9.4	6.9	0.2	13.1	0.2
41.84	70.3	9.2	6.8	0.2	13.2	0.2
52.30	72.0	7.5	5.5	0.2	14.6	0.3

[a]Here, **p1**–**p6** are the C_7H_8 isomers 1,3-heptadien-5-yne (**p1**), toluene (**p2**), 5-methylene-1,3-cyclohexadiene (**p3**), 1,2,4,6-hepatetraene (**p4**), 3-methylene-1-hexen-4-yne (**p5**), and 4-methyl-1,2,3,5-hexatetraene (**p6**).

where only isomers **p3**, **p4**, and **p6** can give hydrogen-loss products, detected at a level of 24 ± 10%, and the combined yield of **p4** and **p6** is calculated to be less than 1% at the experimental collision energy. Note that while the isotopic experiments were unable to fully discriminate between **p1**, **p2**, and **p3**, the experimentally derived branching ratios are consistent with the RRKM calculations and suggest that the reaction mechanism favors the initial formation of intermediate **i1** leading to **p1**, **p2**, **p3**, and possibly **p5**. The addition of 1-propynyl to the terminal position of 1,3-butadiene is favored due to reduced steric hindrance and the relatively high charge density at C1/C4 (0.34) as compared to C2/C3 (0.27) as exemplified in a recent study considering phenyl (C_6H_5) addition to 1,3-butadiene.[53] The reaction pathways leading to the formation of **p1**, **p2**, **p3**, and **p5** are summarized in Figure 12. Considering the results of the RRKM and ab initio calculations, a two-channel fit was produced, accounting for the formation of the theoretically most abundant isomers **p1** and **p2** and is discussed briefly in the Supporting Information.

5. CONCLUSION

The crossed molecular beams method was exploited to explore the formation of C_7H_8 isomers via the reaction of 1-propynyl (CH_3CC; X^2A_1) with 1,3-butadiene ($CH_2CHCHCH_2$; X^1A_g) under single collision conditions. Our data were combined with reactions exploiting (partially) deuterated reactants along with electronic structure and RRKM calculations. Our analysis suggests the formation of the thermodynamically most stable C_7H_8 isomer—toluene ($C_6H_5CH_3$)—via the barrierless addition of 1-propynyl to the 1,3-butadiene terminal carbon atom, forming a low-lying C_7H_9 intermediate that undergoes multiple isomerization steps resulting in cyclization and ultimately aromatization following hydrogen atom elimination. RRKM calculations predict further that the thermodynamically less

DOI: 10.1021/acs.jpca.9b00092
J. Phys. Chem. A 2019, 123, 4104–4118

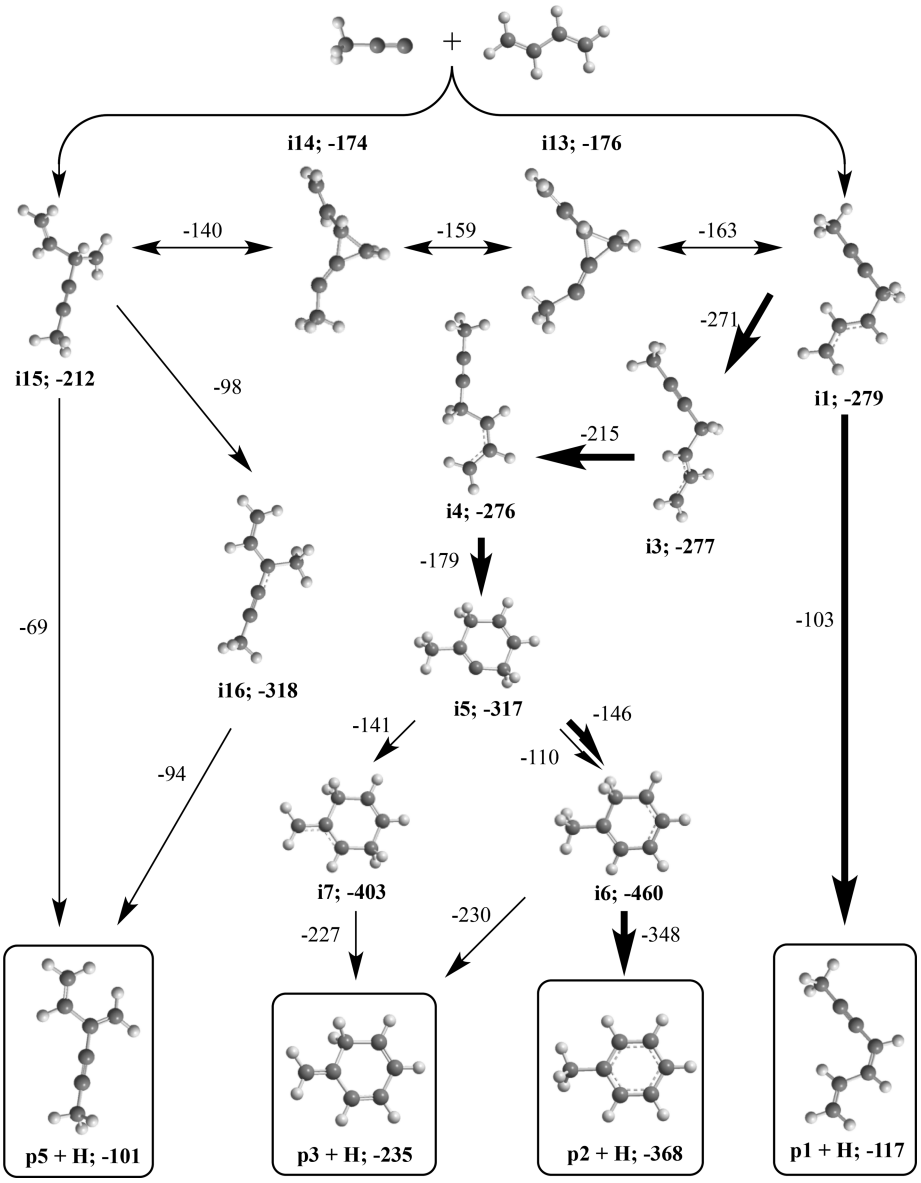

Figure 12. Summary of the most important pathways on the doublet C_7H_9 potential energy surface (Figure 6) leading to C_7H_8 reaction products **p1**, **p2**, **p3**, and **p5** via emission of atomic hydrogen. All energies are given in kJ mol^{-1} relative to the energy of the separated reactants. Arrows of the dominating reaction channels to **p1** and **p2** via **i1** are highlighted in bold.

stable isomers 1,3-heptadien-5-yne, 5-methylene-1,3-cyclohexadiene, and 3-methylene-1-hexen-4-yne are also synthesized. The formation of multiple C_7H_8 isomers as predicted by RRKM studies was confirmed through a series of isotopic experiments that revealed atomic hydrogen is lost from the methylene (CH_2; 61 ± 11%) and methylidyne (CH; 15 ± 15%) groups of 1,3-butadiene and from the methyl (CH_3; 24 ± 10%) group of the 1-propynyl radical. The results presented in this study suggest 1-propynyl could be a key reactant in the synthesis of aromatic molecules that are known precursors to polycyclic aromatic hydrocarbons (PAHs).

PAHs exist throughout the interstellar medium (ISM) as evidenced by the astronomical detection of spectral features in the ultraviolet (UV)[54−56] and infrared (IR)[57,58] regions of the interstellar extinction curve that are reminiscent of the laboratory spectra produced by aromatic hydrocarbons. Despite a rather broad acceptance of an ISM proliferated by PAHs, there has not been a single unambiguous astronomical detection of an individual interstellar PAH in the gas phase. Additional support for the theory comes, however, from two recent discoveries: benzene (C_6H_6), detected in the Westbrook protoplanetary nebular (CRL 618) via IR-active C−H bending,[59] and cyanobenzene (benzonitrile; C_6H_5CN), detected via nuclear (nitrogen) hyperfine splitting in the Taurus Molecular Cloud (TMC-1).[60] Benzene and cyanobenzene have been considered in numerous terrestrial reaction networks under incredibly varied conditions. The most relevant experiments for CRL 618 and TMC-1, considering the low temperatures (C_6H_6 at CRL 618, T = 200 K; C_6H_5CN at TMC-1, T = 7 K) and number densities representative of these environments, are those bimolecular reactions conducted under single collision conditions. Crossed molecular beams experiments have shown that benzene is produced from the reaction of ethynyl (C_2H; $X^2\Sigma^+$) plus 1,3-butadiene,[61] whereas cyanobenzene can form from the reaction of the cyano (CN; $X^2\Sigma^+$) radical with benzene.[62] The theoretical component of these studies suggested that the

DOI: 10.1021/acs.jpca.9b00092
J. Phys. Chem. A 2019, 123, 4104−4118

reactions lack entrance barriers and therefore will proceed spontaneously, in theory, at 0 K, rendering them plausible reaction mechanisms in molecular clouds. Combined with the astronomical detections of cyano and ethynyl radicals, along with the likely presence of 1,3-butadiene in cold molecular clouds,[63] it is clear that single-collision methods are a strong tool for rationalizing the chemistry of extreme environments.

Recently, toluene was identified as a product of the gas phase reaction of ethynyl-*d* (C_2D; $X^2\Sigma^+$) with isoprene (C_5H_8) under single-collision conditions.[27] The reaction mechanism was suggested to proceed barrierlessly and to yield toluene at fractions of up to 52%. The 1-propynyl (CH_3CC) radical could also be present in cold molecular clouds such as TMC-1, resulting from the interaction of UV radiation with the methylacetylene (CH_3CCH) molecule.[64−67] In this way, the CH_3CC radical could serve as a carrier of the methyl group, systematically incorporating itself into methyl-substituted (poly)acetylenes[68−71] or into aromatic systems such as toluene as revealed in this study—where it could represent up to 32% of C_7H_8 products at the low temperature extremes encountered in TMC-1—through a series of bimolecular reactions that are uninhibited by an entrance barrier. Such pathways are a necessary alternative to high energy reactions leading to toluene, such as the addition of the methyl radical to benzene, which has an entrance barrier of 54 kJ mol^{-1} [27] and is therefore closed in the cold regions of space. In summary, we have exposed the reaction dynamics of the formation of toluene ($C_6H_5CH_3$) in a single-collision event of two neutral acyclic reactants, 1-propynyl (CH_3CC) and 1,3-butadiene ($CH_2CHCHCH_2$), in the gas phase. Despite its nondetection outside our solar system, the increasing number of reaction pathways leading to toluene formation encourages a detailed search for its presence among the stars.

■ ASSOCIATED CONTENT

Supporting Information

The Supporting Information is available free of charge on the ACS Publications website at DOI: 10.1021/acs.jpca.9b00092.

Two channel fit, time-of-flight data, laboratory angular distribution, and center-of-mass translational energy and angular flux distributions (PDF)

■ AUTHOR INFORMATION

Corresponding Authors

*(R.I.K.) E-mail: ralfk@hawaii.edu.

*(A.M.M.) E-mail: mebela@fiu.edu.

ORCID

Aaron M. Thomas: 0000-0001-8540-9523

Alexander M. Mebel: 0000-0002-7233-3133

Ralf I. Kaiser: 0000-0002-7233-7206

Notes

The authors declare no competing financial interest.

■ ACKNOWLEDGMENTS

This work was supported by Basic Energy Sciences, U.S. Department of Energy, Grant Nos. DE-FG02-03ER15411 and DE-FG02-04ER15570, to the University of Hawaii and to Florida International University, respectively.

■ REFERENCES

(1) Pelletier, P.-J.; Walter, F. *Ann. Chim. Phys.* **1837**, *67*, 269.

(2) Wilbrand, J. Notiz über Trinitrotoluol. *Justus Liebigs Annalen der Chemie* **1863**, *128*, 178−179.

(3) Chin, J.-Y.; Batterman, S. A. VOC composition of current motor vehicle fuels and vapors, and collinearity analyses for receptor modeling. *Chemosphere* **2012**, *86*, 951−958.

(4) Matsugi, A.; Miyoshi, A. Modeling of two- and three-ring aromatics formation in the pyrolysis of toluene. *Proc. Combust. Inst.* **2013**, *34*, 269−277.

(5) Zhao, L.; Kaiser, R. I.; Xu, B.; Ablikim, U.; Ahmed, M.; Joshi, D.; Veber, G.; Fischer, F. R.; Mebel, A. M. Pyrene Synthesis in Circumstellar Envelopes and its Role in the Formation of 2D Nanostructures. *Nature Astronomy* **2018**, *2*, 413−419.

(6) Zhao, L.; Kaiser, R. I.; Xu, B.; Ablikim, U.; Ahmed, M.; Evseev, M. M.; Bashkirov, E. K.; Azyazov, V. N.; Mebel, A. M. Low-temperature formation of polycyclic aromatic hydrocarbons in Titan's atmosphere. *Nature Astronomy* **2018**, *2*, 973−979.

(7) Yuan, W.; Li, Y.; Dagaut, P.; Yang, J.; Qi, F. Investigation on the pyrolysis and oxidation of toluene over a wide range conditions. I. Flow reactor pyrolysis and jet stirred reactor oxidation. *Combust. Flame* **2015**, *162*, 3−21.

(8) Pelucchi, M.; Cavallotti, C.; Faravelli, T.; Klippenstein, S. J. H-Abstraction reactions by OH, HO_2, O, O_2 and benzyl radical addition to O_2 and their implications for kinetic modelling of toluene oxidation. *Phys. Chem. Chem. Phys.* **2018**, *20*, 10607−10627.

(9) Frenklach, M.; Clary, D. W.; Gardiner, W. C.; Stein, S. E. Detailed Kinetic Modeling of Soot Formation in Shock-Tube Pyrolysis of Acetylene. *Symp. (Int.) Combust., [Proc.]* **1985**, *20*, 887−901.

(10) Parker, D. S. N.; Kaiser, R. I.; Troy, T. P.; Ahmed, M. Hydrogen Abstraction/Acetylene Addition Revealed. *Angew. Chem., Int. Ed.* **2014**, *53*, 7740−7744.

(11) Yang, T.; Troy, T. P.; Xu, B.; Kostko, O.; Ahmed, M.; Mebel, A. M.; Kaiser, R. I. Hydrogen-Abstraction/Acetylene-Addition Exposed. *Angew. Chem., Int. Ed.* **2016**, *55*, 14983−14987.

(12) Cherchneff, I. The Inner Wind of IRC+10216 Revisited: New Exotic Chemistry and Diagnostic for Dust Condensation in Carbon Stars. *Astron. Astrophys.* **2012**, *545*, A12.

(13) Zhao, T. Q.; Li, Q.; Liu, B. S.; Gover, R. K. E.; Sarre, P. J.; Cheung, A. S. C. Laboratory astrochemistry: catalytic conversion of acetylene to polycyclic aromatic hydrocarbons over SiC grains. *Phys. Chem. Chem. Phys.* **2016**, *18*, 3489−3496.

(14) Johansson, K. O.; Head-Gordon, M. P.; Schrader, P. E.; Wilson, K. R.; Michelsen, H. A. Resonance-stabilized hydrocarbon-radical chain reactions may explain soot inception and growth. *Science* **2018**, *361*, 997.

(15) Jin, H.; Frassoldati, A.; Wang, Y.; Zhang, X.; Zeng, M.; Li, Y.; Qi, F.; Cuoci, A.; Faravelli, T. Kinetic Modeling Study of Benzene and PAH Formation in Laminar Methane Flames. *Combust. Flame* **2015**, *162*, 1692−1711.

(16) Sinha, S.; Raj, A. Polycyclic aromatic hydrocarbon (PAH) formation from benzyl radicals: a reaction kinetics study. *Phys. Chem. Chem. Phys.* **2016**, *18*, 8120−8131.

(17) Zhang, L.; Cai, J.; Zhang, T.; Qi, F. Kinetic modeling study of toluene pyrolysis at low pressure. *Combust. Flame* **2010**, *157*, 1686−1697.

(18) Zhang, T.; Zhang, L.; Hong, X.; Zhang, K.; Qi, F.; Law, C. K.; Ye, T.; Zhao, P.; Chen, Y. An experimental and theoretical study of toluene pyrolysis with tunable synchrotron VUV photoionization and molecular-beam mass spectrometry. *Combust. Flame* **2009**, *156*, 2071−2083.

(19) Parker, D. S. N.; Kaiser, R. I.; Kostko, O.; Ahmed, M. Selective Formation of Indene through the Reaction of Benzyl Radicals with Acetylene. *ChemPhysChem* **2015**, *16*, 2091−2093.

(20) Vereecken, L.; Peeters, J. Reactions of chemically activated C9H9 species II: The reaction of phenyl radicals with allene and cyclopropene, and of benzyl radicals with acetylene. *Phys. Chem. Chem. Phys.* **2003**, *5*, 2807−2817.

DOI: 10.1021/acs.jpca.9b00092
J. Phys. Chem. A 2019, 123, 4104−4118

(21) Mebel, A. M.; Landera, A.; Kaiser, R. I. Formation Mechanisms of Naphthalene and Indene: From the Interstellar Medium to Combustion Flames. *J. Phys. Chem. A* **2017**, *121*, 901−926.
(22) Martin, J. W.; Bowal, K.; Menon, A.; Slavchov, R. I.; Akroyd, J.; Mosbach, S.; Kraft, M. Polar curved polycyclic aromatic hydrocarbons in soot formation. *Proc. Combust. Inst.* **2019**, *37*, 1117.
(23) Wu, X.-Z.; Yao, Y.-R.; Chen, M.-M.; Tian, H.-R.; Xiao, J.; Xu, Y.-Y.; Lin, M.-S.; Abella, L.; Tian, C.-B.; Gao, C.-L.; Zhang, Q.; Xie, S.-Y.; Huang, R.-B.; Zheng, L.-S. Formation of Curvature Subunit of Carbon in Combustion. *J. Am. Chem. Soc.* **2016**, *138*, 9629−9633.
(24) Lovas, F. J.; McMahon, R. J.; Grabow, J.-U.; Schnell, M.; Mack, J.; Scott, L. T.; Kuczkowski, R. L. Interstellar Chemistry: A Strategy for Detecting Polycyclic Aromatic Hydrocarbons in Space. *J. Am. Chem. Soc.* **2005**, *127*, 4345−4349.
(25) Kamphus, M.; Braun-Unkhoff, M.; Kohse-Höinghaus, K. Formation of small PAHs in laminar premixed low-pressure propene and cyclopentene flames: Experiment and modeling. *Combust. Flame* **2008**, *152*, 28−59.
(26) Klippenstein, S. J.; Harding, L. B.; Georgievskii, Y. On the formation and decomposition of C_7H_8. *Proc. Combust. Inst.* **2007**, *31*, 221−229.
(27) Dangi, B. B.; Parker, D. S. N.; Kaiser, R. I.; Jamal, A.; Mebel, A. M. A Combined Experimental and Theoretical Study on the Gas-Phase Synthesis of Toluene under Single Collision Conditions. *Angew. Chem.* **2013**, *125*, 7327−7330.
(28) Kaiser, R. I.; Balucani, N.; Charkin, D. O.; Mebel, A. M. A Crossed Beam and Ab Initio Study of the $C_2(X^1\Sigma_g^+/a^3\Pi_u)$ + $C_2H_2(X^1\Sigma_g^+)$ Reactions. *Chem. Phys. Lett.* **2003**, *382*, 112−119.
(29) Balucani, N.; Asvany, O.; Kaiser, R. I.; Osamura, Y. Formation of Three C_4H_3N Isomers from the Reaction of CN ($X^2\Sigma^+$) with Allene, H_2CCCH_2 (XA_1), and Methylacetylene, CH_3CCH (X^1A_1): A Combined Crossed Beam and Ab Initio Study. *J. Phys. Chem. A* **2002**, *106*, 4301−4311.
(30) Kaiser, R. I.; Mebel, A. M.; Chang, A. H. H.; Lin, S. H.; Lee, Y. T. Crossed-Beam Reaction of Carbon Atoms with Hydrocarbon Molecules. V. Chemical Dynamics of n-C_4H_3 Formation from Reaction of $C(^3P_j)$ with Allene, $H_2CCCH_2(X\,^1A_1)$. *J. Chem. Phys.* **1999**, *110*, 10330−10344.
(31) Kaiser, R. I.; Hahndorf, I.; Huang, L. C. L.; Lee, Y. T.; Bettinger, H. F.; Schleyer, P. v. R.; Schaefer, H. F.; Schreiner, P. R. Crossed Beams Reaction of Atomic Carbon, $C(^3P_j)$, with D6-Benzene, $C_6D_6(X\,^1A_{1g})$: Observation of the Per-Deutero-1,2-Didehydro-Cycloheptatrienyl Radical, $C_7D_5(X^2B_2)$. *J. Chem. Phys.* **1999**, *110*, 6091−6094.
(32) Balucani, N.; Mebel, A. M.; Lee, Y. T.; Kaiser, R. I. A Combined Crossed Molecular Beam and ab Initio Study of the Reactions $C_2(X^1\Sigma_g^+, a^3\Pi_u)$ + C_2H_4 → *n*-$C_4H_3(XA')$ + $H(^2S_{1/2})$. *J. Phys. Chem. A* **2001**, *105*, 9813−9818.
(33) Kaiser, R. I.; Maksyutenko, P.; Ennis, C.; Zhang, F.; Gu, X.; Krishtal, S. P.; Mebel, A. M.; Kostko, O.; Ahmed, M. Untangling the Chemical Evolution of Titan's Atmosphere and Surface - From Homogeneous to Heterogeneous Chemistry. *Faraday Discuss.* **2010**, *147*, 429−478.
(34) Thomas, A. M.; Zhao, L.; He, C.; Mebel, A. M.; Kaiser, R. I. A Combined Experimental and Computational Study on the Reaction Dynamics of the 1-Propynyl (CH_3CC)−Acetylene (HCCH) System and the Formation of Methyldiacetylene (CH_3CCCCH). *J. Phys. Chem. A* **2018**, *122*, 6663−6672.
(35) Gu, X.; Guo, Y.; Zhang, F.; Mebel, A. M.; Kaiser, R. I. Reaction dynamics of carbon-bearing radicals in circumstellar envelopes of carbon stars. *Faraday Discuss.* **2006**, *133*, 245−275.
(36) Weiss, P. S. *Reaction Dynamics of Electronically Excited Alkali Atoms with Simple Molecules*. Ph.D. Dissertation; University of California: Berkeley, CA, 1986.
(37) Vernon, M. F. *Molecular Beam Scattering*. Ph.D. Dissertation; University of California: Berkeley, CA, 1983.
(38) Becke, A. D. Density-Functional Thermochemistry. III. The Role of Exact Exchange. *J. Chem. Phys.* **1993**, *98*, 5648−5652.
(39) Lee, C.; Yang, W.; Parr, R. G. Development of the Colle-Salvetti Correlation-Energy Formula into a Functional of the Electron Density. *Phys. Rev. B: Condens. Matter Mater. Phys.* **1988**, *37*, 785−789.
(40) Adler, T. B.; Knizia, G.; Werner, H.-J. A Simple and Efficient CCSD(T)-F12 Approximation. *J. Chem. Phys.* **2007**, *127*, 221106.
(41) Knizia, G.; Adler, T. B.; Werner, H.-J. Simplified CCSD(T)-F12 Methods: Theory and Benchmarks. *J. Chem. Phys.* **2009**, *130*, 054104.
(42) Dunning, T. H. Gaussian Basis Sets for Use in Correlated Molecular Calculations. I. The Atoms Boron through Neon and Hydrogen. *J. Chem. Phys.* **1989**, *90*, 1007−1023.
(43) Werner, H.-J.; Knowles, P.; Lindh, R.; Manby, F. R.; Schütz, M.; Celani, P.; Korona, T.; Rauhut, G.; Amos, R.; Bernhardsson, A. *MOLPRO, Version 2010.1, A Package of Ab Initio Programs*; University of Cardiff: Cardiff, U.K., 2010; see http://www.molpro.net.
(44) Zhang, J.; Valeev, E. F. Prediction of Reaction Barriers and Thermochemical Properties with Explicitly Correlated Coupled-Cluster Methods: A Basis Set Assessment. *J. Chem. Theory Comput.* **2012**, *8*, 3175−3186.
(45) Frisch, M.; Trucks, G.; Schlegel, H.; Scuseria, G.; Robb, M.; Cheeseman, J.; Scalmani, G.; Barone, V.; Mennucci, B.; Petersson, G. *GAUSSIAN 09*, Revision A.1; Gaussian Inc.: Wallingford, CT, 2009.
(46) Robinson, P. J.; Holbrook, K. A. *Unimolecular Reactions*; John Wiley & Sons, Ltd.: New York, 1972.
(47) Eyring, H.; Lin, S. H.; Lin, S. M. *Basic Chemical Kinetics*; John Wiley and Sons, Inc.: New York, 1980.
(48) Steinfield, J.; Francisco, J.; Hase, W. *Chemical Kinetics and Dynamics*; Prentice Hall: Englewood Cliffs, NJ, 1982.
(49) Kislov, V. V.; Nguyen, T. L.; Mebel, A. M.; Lin, S. H.; Smith, S. C. Photodissociation of Benzene under Collision-Free Conditions: An Ab Initio/Rice-Ramsperger-Kassel-Marcus Study. *J. Chem. Phys.* **2004**, *120*, 7008−7017.
(50) Miller, W. B.; Safron, S. A.; Herschbach, D. R. Exchange Reactions of Alkali Atoms with Alkali Halides: A Collision Complex Mechanism. *Discuss. Faraday Soc.* **1967**, *44*, 108−122.
(51) Levine, R. D. *Molecular Reaction Dynamics*; Cambridge University Press: Cambridge, U.K., 2005.
(52) Ruscic, B. *Active Thermochemical Tables*, available at http://atct.anl.gov.
(53) Gu, X.; Zhang, F.; Kaiser, R. I. A Crossed Molecular Beam Study of the Phenyl Radical Reaction with 1,3-Butadiene and its Deuterated Isotopologues. *J. Phys. Chem. A* **2009**, *113*, 998−1006.
(54) Duley, W. W. A Plasmon Resonance in Dehydrogenated Coronene ($C_{24}H_x$) and Its Cations and the Origin of the Interstellar Extinction Band at 217.5 Nanometers. *Astrophys. J.* **2006**, *639*, L59.
(55) Steglich, M.; Jäger, C.; Rouillé, G.; Huisken, F.; Mutschke, H.; Henning, T. Electronic Spectroscopy of Medium-sized Polycyclic Aromatic Hydrocarbons: Implications for the Carriers of the 2175 Å UV Bump. *Astrophys. J., Lett.* **2010**, *712*, L16.
(56) Steglich, M.; Bouwman, J.; Huisken, F.; Henning, T. Can Neutral and Ionized Polycyclic Aromatic Hydrocarbons Be Carriers of the Ultraviolet Extinction Bump and the Diffuse Interstellar Bands? *Astrophys. J.* **2011**, *742*, 2.
(57) Allamandola, L.; Tielens, A.; Barker, J. Interstellar Polycyclic Aromatic Hydrocarbons - The Infrared Emission Bands, the Excitation/Emission Mechanism, and the Astrophysical Implications. *Astrophys. J., Suppl. Ser.* **1989**, *71*, 733−775.
(58) Ricks, A. M.; Douberly, G. E.; Duncan, M. A. The Infrared Spectrum of Protonated Naphthalene and its Relevance for the Unidentified Infrared Bands. *Astrophys. J.* **2009**, *702*, 301−306.
(59) Cernicharo, J.; Heras, A. M.; Tielens, A. G. G. M.; Pardo, J. R.; Herpin, F.; Guélin, M.; Waters, L. B. F. M. Infrared Space Observatory's Discovery of C_4H_2, C_6H_2, and Benzene in CRL 618. *Astrophys. J.* **2001**, *546*, L123−L126.
(60) McGuire, B. A.; Burkhardt, A. M.; Kalenskii, S.; Shingledecker, C. N.; Remijan, A. J.; Herbst, E.; McCarthy, M. C. Detection of the aromatic molecule benzonitrile (C6H5CN) in the interstellar medium. *Science* **2018**, *359*, 202.

DOI: 10.1021/acs.jpca.9b00092
J. Phys. Chem. A 2019, 123, 4104−4118

(61) Jones, B. M.; Zhang, F.; Kaiser, R. I.; Jamal, A.; Mebel, A. M.; Cordiner, M. A.; Charnley, S. B. Formation of Benzene in the Interstellar Medium. *Proc. Natl. Acad. Sci. U. S. A.* **2011**, *108*, 452−457.
(62) Balucani, N.; Asvany, O.; Chang, A. H. H.; Lin, S. H.; Lee, Y. T.; Kaiser, R. I.; Bettinger, H. F.; Schleyer, P. v. R.; Schaefer, H. F. Crossed beam reaction of cyano radicals with hydrocarbon molecules. I. Chemical dynamics of cyanobenzene (C_6H_5CN; X^1A_1) and perdeutero cyanobenzene (C_6D_5CN; X^1A_1) formation from reaction of $CN(X^2\Sigma^+)$ with benzene $C_6H_6(X^1A_{1g})$, and d6-benzene $C_6D_6(X^1A_{1g})$. *J. Chem. Phys.* **1999**, *111*, 7457−7471.
(63) Abplanalp, M. J.; Góbi, S.; Kaiser, R. I. On the formation and the isomer specific detection of methylacetylene (CH_3CCH), propene (CH_3CHCH_2), cyclopropane (c-C_3H_6), vinylacetylene (CH_2CHCCH), and 1,3-butadiene ($CH_2CHCHCH_2$) from interstellar methane ice analogues. *Phys. Chem. Chem. Phys.* **2019**, *21*, 5378.
(64) Harich, S.; Lin, J. J.; Lee, Y. T.; Yang, X. Photodissociation Dynamics of Propyne at 157 nm. *J. Chem. Phys.* **2000**, *112*, 6656−6665.
(65) Sun, W.; Yokoyama, K.; Robinson, J. C.; Suits, A. G.; Neumark, D. M. Discrimination of Product Isomers in the Photodissociation of Propyne and Allene at 193 nm. *J. Chem. Phys.* **1999**, *110*, 4363−4368.
(66) Ganot, Y.; Rosenwaks, S.; Bar, I. H and D Release in ∼ 43.1 nm Photolysis of Vibrationally Excited $3\nu_1$, $4\nu_1$, and $4\nu_{CD}$ Overtones of Propyne-d_3. *J. Chem. Phys.* **2004**, *120*, 8600−8607.
(67) Irvine, W. M.; Hoglund, B.; Friberg, P.; Askne, J.; Ellder, J. The Increasing Chemical Complexity of the Taurus Dark Clouds: Detection of CH_3CCH and C_4H. *Astrophys. J.* **1981**, *248*, L113−L117.
(68) Walmsley, C. M.; Jewell, P. R.; Snyder, L. E.; Winnewisser, G. Detection of Interstellar Methyldiacetylene (CH_3C_4H) in the Dark Dust Cloud TMC 1. *Astron. Astrophys.* **1984**, *134*, L11−L14.
(69) MacLeod, J. M.; Avery, L. W.; Broten, N. W. The Detection of Interstellar Methyldiacetylene (CH_3C_4H). *Astrophys. J.* **1984**, *282*, L89−L92.
(70) Loren, R. B.; Wootten, A.; Mundy, L. G. The Detection of Interstellar Methyl-Diacetylene. *Astrophys. J.* **1984**, *286*, L23−L26.
(71) Remijan, A. J.; Hollis, J. M.; Snyder, L. E.; Jewell, P. R.; Lovas, F. J. Methyltriacetylene (CH_3C_6H) toward TMC-1: The Largest Detected Symmetric Top. *Astrophys. J.* **2006**, *643*, L37−L40.

DOI: 10.1021/acs.jpca.9b00092
J. Phys. Chem. A 2019, 123, 4104−4118